



This discussion paper is/has been under review for the journal Hydrology and Earth System Sciences (HESS). Please refer to the corresponding final paper in HESS if available.

Reconstructing and analyzing China's fifty-nine year (1951–2009) drought history using hydrological model simulation

Z. Y. Wu^{1,2}, G. H. Lu¹, L. Wen³, and C. A. Lin⁴

¹State Key Laboratory of Hydrology-Water Resources and Hydraulic Engineering, Hohai University, Nanjing, China

²College of Hydrology and Water Resources, Hohai University, Nanjing, China

³Department of Atmospheric and Oceanic Sciences, and Global Environmental and Climate Change Centre, McGill University, Montréal, Canada

⁴Atmospheric Science and Technology Directorate, Environment Canada, Montréal, Canada

Received: 27 January 2011 – Accepted: 29 January 2011 – Published: 10 February 2011

Correspondence to: Z. Y. Wu (wzyhhu@gmail.com)

Published by Copernicus Publications on behalf of the European Geosciences Union.

Title Page

Abstract

Introduction

Conclusions

References

Tables

Figures

◀

▶

◀

▶

Back

Close

Full Screen / Esc

Printer-friendly Version

Interactive Discussion

Abstract

The recent fifty-nine year (1951–2009) drought history of China is reconstructed using daily soil moisture values generated by the Variable Infiltration Capacity (VIC) land surface macroscale hydrology model. VIC is applied over a grid of 10 458 points with a spatial resolution of 30 km × 30 km, and is driven by observed daily maximum and minimum air temperature and precipitation from 624 long-term meteorological stations. The VIC soil moisture is used to calculate the Soil Moisture Anomaly Percentage Index (SMAPI), which can be used as a measure of the severity of agricultural drought on a global basis. We develop a SMAPI-based drought identification procedure for practical uses in the identification of both grid point and regional drought events. As the result, a total of 325 regional drought events varying in time and strength are identified from China's nine drought study regions. These drought events can thus be assessed quantitatively at different spatial and temporal scales. The result shows that the severe drought events of 1978, 2000 and 2006 are well reconstructed, indicating SMAPI is capable of indentifying the onset of a drought event, its progressing, as well as its ending. Spatial and temporal variations of droughts on China's nine drought study regions are studied. Our result shows that on average, up to 30% of the total area of China is prone to drought. Regionally, an upward trend in drought-affected areas has been detected in three regions Inner Mongolia, Northeast and North during the recent fifty-nine years. However, the decadal variability of droughts has been week in the rest five regions South, Southwest, East, Northwest, and Tibet. Xinjiang has even been wetting steadily since the 1950s. Two regional dry centers are discovered in China as the result of a combined analysis on the occurrence of drought events from both grid points and drought study regions. The first center is located in the area partially covered by two drought study regions North and Northwest, which extends to the southeastern portion of Inner Mongolia and the southwest part of Northeast. The second one is found in the central to southern portion of the drought study region South. Our study demonstrates the applicability and the value of using modeled soil moisture for reconstructing

Reconstructing and analyzing China's drought history (1951–2009)

Z. Y. Wu et al.

[Title Page](#)

[Abstract](#)

[Introduction](#)

[Conclusions](#)

[References](#)

[Tables](#)

[Figures](#)



[Back](#)

[Close](#)

[Full Screen / Esc](#)

[Printer-friendly Version](#)

[Interactive Discussion](#)

drought histories, and SMAP is useful to analyzing drought at different spatial and temporal scales.

1 Introduction

Drought is one of the major natural disasters that human being has been suffering since the ancient era. Even in nowadays with well developed science and technology, drought is still considered as the most serious hazard to agriculture productions and human lives worldwide. The frequently occurred drought events in recent decades have become major environmental and climatic challenges in the new millennium. With rapid expansion of world population and socioeconomic development, there is an increasing emphasis on the issue of water shortages. With such a shortage of water, the existing drought-affected areas could be further extended. The drought severity would be aggravated too. These will certainly cast shadow on future social and economy developments, which will consequently threaten the well-being of nations and the environment.

Since the most part of continental China is located in the monsoon climate zone, the monthly, annual and inter-annual variations in precipitation and temperature are significant. Thus, large-scale droughts often occur in China. The historical record of droughts shows that China had been hit with 1056 major drought events during the period between 206 BC-1949 AD (or in 2155 years), or having one major drought in every two years in so doing. The drought situation in China has been worsening since the 1950s. The annual average of drought-affected areas has reached 22.5 million hectares, which can account for up to 60% of the total area suffered from natural disasters. The annual average of grain yields lost to droughts is about 12.8 billion kg (Zhang, 2003), which would be enough to feed 85 million people annually. China's drought situation has been further deteriorated since the 1990s. Nationwide droughts occur almost every year (Zou et al., 2005; Zhai et al., 2010; Ma and Ren, 2007; Dai et al., 2004), causing more and more grain yield losses and even threatening the security

Title Page	
Abstract	Introduction
Conclusions	References
Tables	Figures
◀	▶
◀	▶
Back	Close
Full Screen / Esc	
Printer-friendly Version	
Interactive Discussion	

Reconstructing and analyzing China's drought history (1951–2009)

Z. Y. Wu et al.

[Title Page](#)

[Abstract](#)

[Introduction](#)

[Conclusions](#)

[References](#)

[Tables](#)

[Figures](#)



[Back](#)

[Close](#)

[Full Screen / Esc](#)

[Printer-friendly Version](#)

[Interactive Discussion](#)

of drinking water supplies. Drought disasters have become a key factor constraining the sustainable socioeconomic development. Therefore, conducting drought researches and innovating new methodologies to reconstructing historical drought events would enhance our knowledge on drought characteristics, and thus contributing to drought monitoring and prediction.

The popular idea for drought reconstruction is the use of a drought index that can measure the severity of droughts. Because of the complexity of drought and its causing factors, most drought indexes are based on specific geographical and time range (Richard and Heim, 2002), resulting in hundreds of drought indexes for applications around the world (WMO, 1975; Heim, 2000). Most of these indexes are precipitation-based only, as drought is directly caused by the shortage of rainfall, and the precipitation data is easier to obtain than other atmospheric variables (e.g., Raziei et al., 2008). For example, the Palmer Drought Severity Index (PDSI; Palmer, 1965) and the Standardized Precipitation Index (SPI; McKee et al., 1993) are two commonly used indexes of meteorological drought worldwide (e.g., Bordi et al., 2009; Vicente-Serrano and López-Moreno, 2005). Zou et al. (2005) used PDSI to investigate the variations in droughts over China, and Zhai et al. (2010) used both PDSI and SPI to identify tendencies in dry and wet conditions during recent decades over 10 large regions in China. However, Zhai et al. (2010) found that many basins' droughts caused not only by lower precipitation but also by other factors influencing water balance conditions. In fact, for agriculture, the first sector to be affected by the onset of droughts (Narasimhan and Srinivasan, 2005), soil moisture is more crucial than precipitation. Sufficient water supply is essential for the growth of crops at different stages. The crop production is thus strongly influenced by soil moisture conditions. According to the World Meteorological Organization (WMO, 1975), the agriculture drought relates to a shortage of available water for plant growth, and is assessed as insufficient soil moisture to replace evapotranspirative losses. Having accurate soil moisture information is thus essential and important to assessing and predicting agricultural droughts.

Reconstructing and analyzing China's drought history (1951–2009)

Z. Y. Wu et al.

[Title Page](#)[Abstract](#)[Introduction](#)[Conclusions](#)[References](#)[Tables](#)[Figures](#)[Back](#)[Close](#)[Full Screen / Esc](#)[Printer-friendly Version](#)[Interactive Discussion](#)

Reconstructing and analyzing China's drought history (1951–2009)

Z. Y. Wu et al.

[Title Page](#)[Abstract](#)[Introduction](#)[Conclusions](#)[References](#)[Tables](#)[Figures](#)[◀](#)[▶](#)[◀](#)[▶](#)[Back](#)[Close](#)[Full Screen / Esc](#)[Printer-friendly Version](#)[Interactive Discussion](#)

establishment of daily drought index. The hydrological model-based soil moisture approach is thus suitable for analyzing the drought occurrence and intensity at different spatial and temporal scales.

The VIC (Variable Infiltration Capacity) model (Liang et al., 1994, 1996) is such a land surface macroscale hydrology model that has been widely used (Lobmeyr et al., 1999; te Linde et al., 2008; Stephen et al., 2010). It uses a spatial probability distribution function to represent subgrid variability in soil moisture storage capacity. Such a function is used in Xinanjiang model (Zhao et al., 1980), Hamburg Climate Model (Dümenil et al., 1992), Interface Soil Biosphere Atmosphere model (Habets et al., 1999), and Canadian Land Surface Scheme (CLASS; Verseghy, 1991; Verseghy et al., 1993; Wen et al., 2007) for calculating saturation excess runoff, and the General Runoff Yield model (Wen et al., 1982) for generating infiltration excess runoff. The function is designed to take into account heterogeneity of land surface properties, and can give more realistic treatment of hydrological processes within a model grid cell. Nijssen et al. (2001) used VIC to generate 14 years (1980–1993) of global daily soil moisture at a resolution of $2^\circ \times 2^\circ$. Andreadis et al. (2005) reconstructed the drought history of the continental US from 1920 to 2003 based upon VIC soil moisture and runoff at a resolution of $0.5^\circ \times 0.5^\circ$. Wu et al. (2007) recently applied VIC to generate 35 years (1971–2005) of daily soil moisture over China at a resolution of $30 \text{ km} \times 30 \text{ km}$.

The soil moisture dataset used in this study is derived from a newly-completed multi-year VIC simulation, which extends the simulation period from previous thirty-five years (1971–2005; Wu et al., 2007) to current fifty-nine years (1951–2009). The VIC moisture is used to calculate the Soil Moisture Anomaly Percentage Index (SMAPI; Bergman et al., 1988), which can be used as a measure of the severity of agricultural droughts. The details of SMAPI will be discussed in the later section. The calculated SMAPI is ultimately used to quantify the most documented drought events in the recent fifty-nine years in China.

2 Data and methodology

2.1 VIC soil moisture simulation

Technically speaking, VIC is applied over a grid of 10 458 points with a spatial resolution of 30 km × 30 km. VIC has four types of user defined parameters: soil, vegetation, hydrology, and “catchment definition”. By the latter, we mean basin characteristics (latitude, longitude, elevation) and climate parameters (time average near surface air temperature and precipitation). For each grid point, the global 10-km soil profile dataset (Reynolds et al., 2000) and the global 1-km land cover classification dataset (Hansen et al., 2000) are used to define the model soil and vegetation parameters. The catchment parameters of VIC are determined using the Global 30 Arc-Second Elevation Data Set from the US Geological Survey, and the observed time average near-surface air temperatures and precipitation. Three soil layers are used in the model simulation with the top layer being fixed at 0.1 m depth. The depths of the second and third layer are adjustable, which are determined by the model calibration process. The regression relations between the VIC hydrological parameters and the catchment climate characteristics are used for the parameter determination over ungauged catchments, which are detailed in Wu et al. (2007).

VIC is driven by observed daily maximum and minimum air temperature and precipitation from 624 long-term meteorological stations in China. This continually updated meteorological dataset has been available since 1 January 1951 and is quality-controlled. The daily meteorological observations are interpolated onto each of the 10 458 grid points using the inverse distance weighted method. VIC is then applied on each grid point for the calculation of surface water balance using a daily time step. The energy balance is not considered as long-term and nationwide observations of short-wave radiation are not available. The climatology of 1 January soil moisture over the period of 1951–2009 is used as the initial soil moisture value for VIC to generating the soil moisture dataset.

[Title Page](#)[Abstract](#)[Introduction](#)[Conclusions](#)[References](#)[Tables](#)[Figures](#)[◀](#)[▶](#)[Back](#)[Close](#)[Full Screen / Esc](#)[Printer-friendly Version](#)[Interactive Discussion](#)

Reconstructing and analyzing China's drought history (1951–2009)

Z. Y. Wu et al.

[Title Page](#)

[Abstract](#)

[Introduction](#)

[Conclusions](#)

[References](#)

[Tables](#)

[Figures](#)

◀

▶

[Back](#)

[Close](#)

[Full Screen / Esc](#)

[Printer-friendly Version](#)

[Interactive Discussion](#)



VIC is first calibrated using observed hydrographs from 35 catchments with drainage areas varying from 190 to 351 530 km². The VIC model is then validated over these 35 catchments at different periods and over an additional eight catchments with drainage areas ranging from 1230 to 10 010 km². In situ soil moisture measurements from 28 sites around China are also used for model validation. VIC performs well over both calibration and validation catchments especially in humid and semi-humid regions, and detailed VIC calibration and validation are discussed and provided in Wu et al. (2007). For example, the overall average values of correlation coefficient of simulated and observed soil moisture anomalies for the 28 sites are 0.60, 0.50 and 0.52 for depths of 0–20, 20–100 and 0–100 cm, respectively, indicating satisfactory model performance on soil moisture simulation. Also, the 59-year soil moisture climatology for the top 1 m from VIC is consistent with known soil moisture conditions in China, illustrating the ability of VIC model in reproducing large spatial scale characteristics of soil moisture over a long period of time. Therefore, our current study is a continuation of the study of Wu et al. (2007), with the emphasis on the analysis and application of the simulated long-term soil moisture products.

2.2 Soil moisture anomaly percentage index (SMAPI)

The precise quantification of a drought event is a classical issue and difficult challenge in geosciences. Several specialized drought indices have been proposed to describe four major types of drought: meteorological, hydrological, agricultural and socio-economic (Heim, 2000). The latter form can be considered the consequence of the other three physical types of drought. A useful survey on drought indices is found in WMO (1975) and Heim (2000). Keyantash and Dracup (2002) evaluated the most prominent indices that measure each of the three physical types of drought using a set of six weighted decision criteria: robustness, tractability, transparency, sophistication, expendability, and dimensionality. The performance of each of the 14 evaluated drought indices is measured with an assigned value from 1 to 5 (5 being the highest). The average value of the six criteria is 3 for the Soil Moisture Anomaly Percentage

Index (SMAPI) proposed by Bergman et al. (1988), which is second highest among the five evaluated indices for agricultural drought.

SMAPI is developed to characterize agricultural drought over a large area. The approach of SMAPI to defining drought severity is through a measurement on the relative departure of soil moisture from the normal climate at a specific grid point or region. In this study, SMAPI is used as a measure of agricultural drought, which is defined as:

$$\text{SMAPI} = \frac{\theta - \bar{\theta}}{\bar{\theta}} \times 100\% \quad (1)$$

where, θ and $\bar{\theta}$ represent the current value of soil moisture and its climatology, respectively. Bergman et al. (1988) reported that SMAPI values change at a rate centered between the rapid Crop Moisture Index (CMI; Palmer, 1968) and the relatively slow Palmer Drought Severity Index (PDSI; Palmer, 1965). The rationale of using the relative soil moisture deficit rather than the absolute magnitude is because anomalies in absolute terms reflect different severities in different parts of a studying domain. The absolute soil moisture deficit is thus not appropriate for the purpose of comparing drought severities at different grid points in this study.

The drought (or wet) classification based on the SMAPI was studied prior to the current study. We calculated SMAPI values using observed soil moisture collected on the 1st, 11th, and 21st of every month from 1981 to 1999 at 10 experimental sites located in different regions of China. Figure 1 shows the frequency distributions of SMAPI for the 10 sites, as well as their average. Obviously, the latter pattern can be represented by a Gaussian distribution. SMAPI can thus be used to compare droughts in different regions. Based on analysis of drought data from the 10 sites, SMAPI values can be classified into nine categories as shown in Table 1. Our proposed categories are similar to that of Palmer (1965).

Reconstructing and analyzing China's drought history (1951–2009)

Z. Y. Wu et al.

[Title Page](#)

[Abstract](#)

[Introduction](#)

[Conclusions](#)

[References](#)

[Tables](#)

[Figures](#)



[Back](#)

[Close](#)

[Full Screen / Esc](#)

[Printer-friendly Version](#)

[Interactive Discussion](#)

2.3 SMAPI-based identification of drought events

A drought event can be characterized by its duration, intensity, severity and areal extent. We propose a SMAPI-based drought identification procedure for practical uses in the identification of both grid point and regional drought events, which can be explained as follow.

For a grid point, we define the drought duration as the number of consecutive days with SMAPI values below -5% , while their average is called the drought intensity. The drought severity is the product of drought intensity and the drought duration. We use 60 days as the minima threshold for the drought duration to qualifying a drought event at the grid point scale.

The areal extent of droughts is an important feature to identifying large-scale drought events. For a drought study region, we define the daily areal extent as the percentage of the total grid points with SMAPI values below -5% . The daily drought intensity of a region refers to the average of SMAPI values of all grid points covered by the region. Differing from the situation for a grid point, the drought duration of a region is defined as the number of consecutive days with values of the daily areal extent greater than 30%. Similar to a grid point, the drought severity of a region is the product of daily drought intensity of that region and its drought duration. We also use 60 days as the minima threshold for the drought duration to qualifying a drought event at the regional scale.

2.4 China's nine drought study regions

China covers a vast area of 9.6 million square kilometers, and is known to its diversified landscapes with plateaus and mountains in the west and lower lands on the east. China climate varies radically from north to south as well as from west to east, it crosses five temperature zones. Precipitation in China increases from northwest to southeast, with significant variations in annual amounts. As a result, China is divided into nine drought study regions by Chinese Ministry of Water Resources (CMWR, 1997). Such

[Title Page](#)

[Abstract](#)

[Introduction](#)

[Conclusions](#)

[References](#)

[Tables](#)

[Figures](#)

◀

▶

◀

▶

[Back](#)

[Close](#)

[Full Screen / Esc](#)

[Printer-friendly Version](#)

[Interactive Discussion](#)



[Title Page](#)[Abstract](#)[Introduction](#)[Conclusions](#)[References](#)[Tables](#)[Figures](#)[◀](#)[▶](#)[◀](#)[▶](#)[Back](#)[Close](#)[Full Screen / Esc](#)[Printer-friendly Version](#)[Interactive Discussion](#)

division scheme is adapted in this study to preserving a consistency among regional drought studies, as well as the convention in geographical naming. Figure 2 shows the geographical distribution of these nine drought study regions, which are Xinjiang, Tibet, Northwest, Inner Mongolia, Northeast, North, East, Southwest and South. Each 5 region includes at least one of the 31 provinces in mainland China.

3 Result

3.1 Annual cycle of soil moisture

The annual cycle of VIC soil moisture in the top 1-m column are shown in Fig. 3. Each 10 panel of the figure represents the annual time series of spatially-averaged soil moisture, precipitation and evapotranspiration on one of the nine drought study regions in China. The three climatologies are the averages of a 59-year period from 1 January 1951 to 31 December 2009. The result shows that the annual variation in soil moisture on these regions is evidently different from each other, varying from high values with 15 a considerable seasonality in South to very low values having almost no seasonality in Xinjiang. The overall annual variation in soil moisture corresponds well with the observed precipitation gradient crossing China as shown in Fig. 3.

On the nine drought study regions, the annual cycle of soil moisture can be further aggregated into three categories. Xinjiang, Tibet and Northwest form the first category, which can be characterized as regions with low soil moisture values and small seasonalities. The second one involves Inner Mongolia, North and Northeast three regions with 20 low soil moisture values and moderate seasonal variations. In this category, the water storage in soil column is depleted during spring seasons and will be recharged in summers. The maximum value of soil moisture is usually observed in late summers, while the minimum one being in early summers. The soil moisture value remains almost constant during autumn and winter seasons. The third category includes Southwest, 25 South and East. High soil moisture values and notable seasonal variations are main

characteristics observed on these three humid regions. The regions are covered by the East Asian monsoon area that is characterized by a warm and wet summer and a cold and dry winter. The soil moisture in the regions can be recharged in the warm season and will be depleted in the cold season. The annual cycle of soil moisture is largely influenced by monsoon activities. The occurrences of soil moisture maximum and minimum are different over the three humid regions, which are in August and April over Southwest, in June and December over South, and in May and October over East, respectively. Our proposed three categories are consistence with other drought studies (Zhang et al., 2008b; Zhang, 2009).

10 3.2 Identification of regional historical drought events

We apply the SMPI-based drought identification procedure to China to identifying regional drought events over a 59-year period commencing on 1 January 1951, and ending on 31 December 2009. The SMPI threshold is set to -5% in this study, which is the upper limit of mild droughts in Table 1. A total of 325 regional historical drought events varying in time and strength are identified from China's nine drought study regions. Table 2 summarizes the result of those identified events from the nine regions.

Our study reveals that the regions with the most frequent drought-hit are found in South and North as shown in the second column of Table 2. Both regions experienced 53 regional drought events in the recent fifty-nine years, and then followed by East with 46 events. Over each region, the top three most severe drought events are given in the last three columns of table after examining the drought severity among the identified events. The beginning and ending dates of a drought event (T_1/T_2), the drought duration (D), and the drought areal extent (A) are also listed in the columns. The drought severity is defined as the product of drought intensity and the drought duration, which is discussed in the last section. On average, the drought duration in North is about three times longer than that in South, although the two regions were hit with the same number of drought events. The region with the least number of drought events is found in Xinjiang, over which only six drought events have been identified in the recent fifty-nine

Title Page	
Abstract	Introduction
Conclusions	References
Tables	Figures
	
Back	Close
Full Screen / Esc	
Printer-friendly Version	
Interactive Discussion	

Reconstructing and analyzing China's drought history (1951–2009)

Z. Y. Wu et al.

[Title Page](#)

[Abstract](#)

[Introduction](#)

[Conclusions](#)

[References](#)

[Tables](#)

[Figures](#)



[Back](#)

[Close](#)

[Full Screen / Esc](#)

[Printer-friendly Version](#)

[Interactive Discussion](#)

years. The drought duration in Xinjiang is also relatively shorter comparing to that in other regions.

The analysis has been carried out on the 27 most severe drought events identified from the nine drought study regions. The three drought parameters T_1/T_2 , D , and

5 A provided in Table 2 are quantitatively compared with the drought records officially released by the Chinese authorities. The result shows that these identified drought

events are in good agreements with the corresponding records most of the case. For example, the first ranking event of East was from 16 June 1978 to 6 May 1979. The drought parameters duration (D) and areal extent (A) are 325 days and 68.9% respectively as shown in Table 2. This identified event is well reported in the China Historical Drought 1949–2000 (Zhang et al., 2008a), “the severe drought of 1978–1979 in Eastern China resulted in a direct loss of 20.1 million tons in grain productions”.

10 The second ranking event of Northeast was from 14 August 1977 to 19 April 1979, and having a 614-day duration and 54.5% areal extent. The corresponding record (Zhang et al., 2008a) showed that a total of 14.6 billion Yuan was lost to the severe drought

15 event of 1977–1979 in Northeast China. In 2000, a series of unprecedented droughts hit China nationwide. The drought caused a gain loss of 59.96 million tons, which has made the year 2000 as the most severe drought year since 1949 (Zhang et al., 2008a). The result of the 27 most severe drought events in Table 2 indicates that there were

20 three first ranking drought events involving the most severe drought year 2000. The 757-day long event on Northeast was from 24 May 2000 to 19 June 2002. The 788-day long on North was 27 August 1998 to 22 October 2000; and the 1063-day long on Inner Mongolia was 14 July 1999 to 10 June 2002. These three drought study regions also cover a large portion of China's cultivated lands. Another record breaking drought

25 event occurred in Chongqing in 2006, which resulted in a severe shortage of drinking water. Chongqing is one of the four municipalities with a population of over 30 million people and is the largest city in Western China. The 2006 severe drought had affected more than 21 million people's life in Chongqing, and two-thirds of its river systems had dried up (Hao et al., 2007). This event is also well reconstructed in this study (Table 2),

as Chongqing was suffered from a 232-day long severe drought event that was first ranking on Southwest. This event began on 15 June 2006 and ended on 1 February 2007.

3.3 Spatial extension and variation of droughts in China

- 5 The spatial extension and variation of droughts on China's nine drought study regions are studied. We show in Fig. 4 four reconstructed severe drought events together with other drought-affected areas for the same events to illustrate the drought spatial distribution and extension at both regional and continental scales. All four are ranking first regional events in terms of the drought severity as indicated in Table 2, and they were
10 varying in time and strength, and occurred on four drought study regions South, East, Inner Mongolia, and Southwest. Other areas (or grid points) in China with SMAPI values below -5% for the same drought events are also shown on each of the four panels of Fig. 4. This should give us a nationwide complete picture of the drought-affected areas during the episode of four regional drought events, as a large scale severe drought
15 is most likely not an isolated incident. For example, during the occurrence of the 325-day long event on East (Fig. 4b), portions of other two drought study regions Northeast and the North were also suffered from droughts during the same 325-day period. This common feature is observable in other three panels of Fig. 4.

- Over a region, the severity of a drought event is usually not uniformly distributed.
20 Local convergences of a large scale drought event are commonly recognized in many drought studied. This local convergence is also well reconstructed in this study, and many of them are coincident well with the drought records officially released by authorities. Exception is found on the drought study region South as shown in Fig. 4d, where the severe drought almost extended to the entire region during the episode of
25 the 254-day long event.

At a grid point scale, the long-term drought occurrence on each of the 10 458 VIC grid points in China is examined using the SMAPI-based drought identification procedure over the period 1 January 1951 to 31 December 2009. For example, a maximum of 62

Title Page	
Abstract	Introduction
Conclusions	References
Tables	Figures
◀	▶
◀	▶
Back	Close
Full Screen / Esc	
Printer-friendly Version	
Interactive Discussion	

Reconstructing and analyzing China's drought history (1951–2009)

Z. Y. Wu et al.

[Title Page](#)

[Abstract](#)

[Introduction](#)

[Conclusions](#)

[References](#)

[Tables](#)

[Figures](#)



[Back](#)

[Close](#)

[Full Screen / Esc](#)

[Printer-friendly Version](#)

[Interactive Discussion](#)

drought events has been identified from a grid point that is happened to be bordered by two drought study regions North and East. Figure 5 shows the geographic distribution of drought occurrences over China in the recent fifty-nine years. The drought distribution with different strengths is generally found in most regions of China. However, the drought frequency exhibits a diversified characteristic ranging from less occurring in the West to very common in the East. The latter poses a serious threat to China as the most Country's social-economical activities are concentrated in the East. Two regional dry centers are clearly shown in the figure. This discovery is further supported by the analysis of the drought occurrence on the nine drought study regions. The first center is located in the area partially covered by two drought study regions North and Northwest, which extends to the southeastern portion of Inner Mongolia and the southwest part of Northeast. The second one is found in the central to southern part of the drought study region South. The drought occurrence in China East is largely influenced by the location and strength of the western Pacific subtropical high as well as the development of the westerly circulation.

The decadal variation in the drought occurrence at each grid point is analyzed. We show in Fig. 6 six geographic distributions of drought occurrences over China in the recent six decades (1951–1959, 1960–1969, 1970–1979, 1980–1989, 1990–1999 and 2000–2009). Each panel of the figure represents the drought occurrences in one decade. The nationwide decadal variation of drought occurrences can thus be seen clearly from the six panels of Fig. 6. For example, the drought occurrence in China had been fairly moderate in the first three decades until the end of the 70's, as the grid points with 8 or more accumulated drought events per decade are rare. There were scattered grid points hit by multiple drought events. The large-scale and long-term trend in drought occurrences is found to be insignificant. However, the situation has been changed dramatically in last three decades beginning in the early 80's. There has been a significant increase in the number of grid points with 8 or more accumulated drought events per decade, and they appeared to be more organized, structured and regionally concentrated. This regional concentration was clearly evident on the entire

Reconstructing and analyzing China's drought history (1951–2009)

Z. Y. Wu et al.

[Title Page](#)[Abstract](#)[Introduction](#)[Conclusions](#)[References](#)[Tables](#)[Figures](#)[◀](#)[▶](#)[◀](#)[▶](#)[Back](#)[Close](#)[Full Screen / Esc](#)[Printer-friendly Version](#)[Interactive Discussion](#)

drought study region North in the 1980s. Over the next two decades, the regional concentration was first developed westward to the drought study region Northwest in the 1990s, and then further extended northeastward to a large portions of the drought study region Inner Mongolia and almost entire Northwest in the 2000s. Another smaller center has been growing steadily since the 1960s, and extended to a large area of the drought study regions South in the 2000s. The overall result indicates that the drought situation has been worsening in China especially in the most social-economical concentrated areas since the 1980s. This finding on drought decadal variations is in good qualitative agreement with observations and many other drought reports released by authorities at different levels in China.

3.4 Trends in the recent 59-year drought over China's nine drought study regions

Drought is a regional phenomenon with high spatial and temporal variability. Droughts are recurring aspects of weather and climate extremes. Trends in the recent 59-year drought over China's nine drought study regions are studied. We show in Fig. 7 the time series of monthly areal extents of droughts on each drought study region with the trend lines. The definition of daily drought areal extent is provided in the last section, which is seen as the percentage of the total grid points with SMAPI values below -5% over a drought study region. The monthly areal extent of droughts can thus be calculated based on daily values. As shown in Fig. 7, three drought study regions Inner Mongolia, Northeast and North exhibit an upward trend, while only one region Xinjiang trended downward, and almost no trend can be observed from the rest five regions Tibet, Northwest, East, Southwest and South. The 59-year average in monthly areal extents of droughts has increased by almost 30% in these three upward regions, while this statistic was only -17% for the downward region Xinjiang and within $\pm 10\%$ for the rest five regions. It is important to note that there seems to be a sudden upward jump in the monthly areal extent of droughts in Inner Mongolia during the last ten years.

Monthly, annual, inter-annual variations of droughts are clearly evident on most of the nine drought study regions as shown in Fig. 7. The regional difference in these variations is observable. The most active regions with high variability in the monthly areal extent of drought are found to be in East, Southwest and South. For example,

5 the drought-affected area was less than 10% on the drought study region South in September 1979; however, this number was quickly increased to over 95% in January 1980 in just four months. The frequency of these variations tends to be speeded-up in recent two decades.

The decadal trend in the areal extent of droughts is quantitatively studied over
10 China's nine drought study regions. The decadal areal extent of droughts is calculated based on daily values. We show in Fig. 8 the decadal average of drought area percentages on the nine drought study regions Xinjiang, Tibet, Northwest, Inner Mongolia, Northeast, North, East, Southwest and South in the recent six decades (1951–1959, 1960–1969, 1970–1979, 1980–1989, 1990–1999 and 2000–2009). On average, up to
15 30% of the total area of China is prone to drought, and this finding is consistent with the conclusion from another study based on the calculated Palmer Drought Severity Index (PDSI) using observed precipitation and temperature (Zou et al., 2005). The spatial and temporal variability is observed among regional changes in drought areal extents in the recent six decades. Regionally, an upward trend in drought-affected areas has
20 been detected in three regions North, Northeast and Inner Mongolia especially during the last 30 years as shown in Fig. 8. Over North, more than 50% of the area had been affected by droughts during the past three decades (1980s, 1990s and 2000s), and this finding is also in good agreement with other two studies (Wang and Zhai, 2003; Zou et al., 2005). For example, Wang and Zhai (2003) revealed an expanding trend of drought
25 areas in northern major agricultural areas in the last fifty years using the China-Z index, while Zou et al. (2005) obtained the similar trend using the PDSI index, and our study confirms these observations. However, the decadal variability of droughts has been week in the rest five regions South, Southwest, East, Northwest, and Tibet. Xinjiang has even been wetting steadily since the 1950s, which is also reported by Ma and Fu

Reconstructing and analyzing China's drought history (1951–2009)

Z. Y. Wu et al.

[Title Page](#)

[Abstract](#)

[Introduction](#)

[Conclusions](#)

[References](#)

[Tables](#)

[Figures](#)



[Back](#)

[Close](#)

[Full Screen / Esc](#)

[Printer-friendly Version](#)

[Interactive Discussion](#)

4 Conclusions

We have used the VIC land surface macroscale hydrology model to reconstruct China's daily soil moisture values from 1 January 1951 to 31 December 2009, at a spatial resolution of 30 km × 30 km. VIC is applied over a grid of 10 458 points, and is driven by observed daily maximum and minimum air temperature and precipitation from 624 long-term meteorological stations. VIC performs well over both calibration and validation catchments especially in humid and semi-humid regions, and detailed VIC calibration and validation are found in Wu et al. (2007). This newly-completed multiyear VIC simulation has extended the simulation period from previous thirty-five years (1971–2005; Wu et al., 2003) to current fifty-nine years (1951–2009), and can thus provide us with a 59-year soil moisture dataset for this study.

The VIC soil moisture is used to calculate the Soil Moisture Anomaly Percentage Index (SMAPI), which can be used as a measure of the severity of agricultural drought on a global basis. We develop a SMAPI-based drought identification procedure for practical uses in the identification of both grid point and regional drought events. As the result, a total of 325 regional drought events varying in time and strength are identified from China's nine drought study regions Xinjiang, Tibet, Northwest, Inner Mongolia, Northeast, North, East, Southwest and South. The result shows that the severe drought events of 1978, 2000 and 2006 are well reconstructed, indicating SMAPI is capable of identifying the onset of a drought event, its progressing, as well as its ending.

The identified drought events have been assessed quantitatively at different spatial and temporal scales. Results show that on average, up to 30% of the total area of China is prone to drought. The drought frequency exhibits a diversified characteristic ranging from less occurring in the West to very common in the East. Regionally, an upward trend in drought-affected areas has been detected in three regions Inner Mongolia,

Reconstructing and analyzing China's drought history (1951–2009)

Z. Y. Wu et al.

[Title Page](#)

[Abstract](#)

[Introduction](#)

[Conclusions](#)

[References](#)

[Tables](#)

[Figures](#)

◀

▶

◀

▶

[Back](#)

[Close](#)

[Full Screen / Esc](#)

[Printer-friendly Version](#)

[Interactive Discussion](#)



Reconstructing and analyzing China's drought history (1951–2009)

Z. Y. Wu et al.

[Title Page](#)

[Abstract](#)

[Introduction](#)

[Conclusions](#)

[References](#)

[Tables](#)

[Figures](#)

◀

▶

[Back](#)

[Close](#)

[Full Screen / Esc](#)

[Printer-friendly Version](#)

[Interactive Discussion](#)



Northeast and North during the last fifty-nine years. The 59-year average in monthly areal extents of droughts has increased by almost 30% in these three upward regions, while this statistic was only –17% for the downward region Xinjiang and within ±10% for the rest five regions. It is important to note that there seems to be a sudden upward jump in the monthly areal extent of droughts in Inner Mongolia during the last ten years. Two regional dry centers are discovered in China as the result of a combined analysis on the occurrence of drought events from both grid points and drought study regions. The first center is located in the area partial covered by two drought study regions North and Northwest, which extends to the southeastern portion of Inner Mongolia and the southwest part of Northeast. The second one is found in the central to southern portion of the drought study region South. Our study demonstrates the applicability and the value of using modeled soil moisture for reconstructing drought histories, and SMAPI is useful to analyzing drought at different spatial and temporal scales. The SMAPI-based methodology would be applicable for real time drought monitoring and forecasting when meteorological forecasts being provided, as our VIC soil moisture simulation emphasizes on the idea of maintaining consistency between the real time and long-term soil moisture simulations.

Based on the current study, the following recommendations are generally intended for future VIC studies in China. First, it would be desirable to having additional observed meteorological variables, which will help to reduce the uncertainty in model inputs. Second, we will increase the number of VIC calibration and validation catchments, in particular those with a large catchment size. Third, we will improve the form of the spatial probability function currently being used in VIC to better represent the sub-grid variability in soil moisture storage capacity.

Acknowledgements. This work is supported by the National Natural Science Foundation of China (grant No. 41001012), the National Basic Research Program of China (973 Program) (grant No. 2010CB428405), the Special Public Sector Research Program of Ministry of Water Resources (Grant No. 200701039) and the Fundamental Research Funds for the Central Universities (Grant No. 2009B00114).

References

Reconstructing and analyzing China's drought history (1951–2009)

Z. Y. Wu et al.

- Albergel, C., Calvet, J.-C., de Rosnay, P., Balsamo, G., Wagner, W., Hasenauer, S., Naeimi, V., Martin, E., Bazile, E., Bouyssel, F., and Mahfouf, J.-F.: Cross-evaluation of modelled and remotely sensed surface soil moisture with in situ data in southwestern France, *Hydrol. Earth Syst. Sci.*, 14, 2177–2191, doi:10.5194/hess-14-2177-2010, 2010.
- Andreadis, K. M., Clark, E. A., Wood, A. W., Hamlet, A. F., and Lettenmaier, D. P.: Twentieth-century century drought in the conterminous United States, *J. Hydrometeorol.*, 6, 985–1001, 2005.
- Bergman, K. H., Sabol, P., and Miskus, D.: Experimental indices for monitoring global drought conditions, in: Proc. 13th Annual Climate Diagnostics Workshop, Cambridge, MA, US Dept. of Commerce, 190–197, 1988.
- Bordi, I., Fraedrich, K., and Sutera, A.: Observed drought and wetness trends in Europe: an update, *Hydrol. Earth Syst. Sci.*, 13, 1519–1530, doi:10.5194/hess-13-1519-2009, 2009.
- Dai, A. G., Trenberth, K. E., and Qian, T. T.: A global dataset of palmer drought severity index for 1870–2002: relationship with soil moisture and effects of surface warming, *J. Hydrometeorol.*, 5, 1117–1130, 2004.
- Dümenil, L. and Todini, E.: A rainfall-runoff scheme for use in the Hamburg climate model, in: Advances in Theoretical Hydrology, a Tribute to James Dooge, edited by: O'Kane, J., European Geophysical Society Series in Hydrological Sciences, 1, Elsevier, Amsterdam, 129–157, 1992.
- Gray, D. M.: Handbook on the Principles of Hydrology, Water Information Center, NY, 1970.
- Habets, F., Noilhan, J., Golaz, C., Goutorbe, J. P., Lacarrère, P., Leblois, E., Ledoux, E., Martin, E., Ottlé, C., and Vidal-Madjar, D.: The ISBA surface scheme in a macroscale hydrological model applied to the Hapex-Mobilhy area Part 1: Model and database, *J. Hydrol.*, 217, 75–96, 1999.
- Hansen, M. C., DeFries, R. S., Townshend, J. R. G., and Sohlberg, R.: Global land cover classification at 1 km spatial resolution using a classification tree approach, *Int. J. Remote Sens.*, 21, 1331–1364, 2000.
- Hao, Z. X., Ge, Q. S., Zhen, J. Y., and Li, Y. Q.: 2006 extreme drought event of Chongqing, *Geogr. Res.*, 26, 828–834, 2007.
- Heim, R. R.: Drought indices: a review, in: Drought: A Global Assessment, edited by: Wilhite, D. A., Routledge, 159–167, 2000.

[Title Page](#)

[Abstract](#)

[Introduction](#)

[Conclusions](#)

[References](#)

[Tables](#)

[Figures](#)



[Back](#)

[Close](#)

[Full Screen / Esc](#)

[Printer-friendly Version](#)

[Interactive Discussion](#)



Reconstructing and analyzing China's drought history (1951–2009)

Z. Y. Wu et al.

[Title Page](#)

[Abstract](#)

[Introduction](#)

[Conclusions](#)

[References](#)

[Tables](#)

[Figures](#)

◀

▶

◀

▶

[Back](#)

[Close](#)

[Full Screen / Esc](#)

[Printer-friendly Version](#)

[Interactive Discussion](#)



- Juglea, S., Kerr, Y., Mialon, A., Lopez-Baeza, E., Braithwaite, D., and Hsu, K.: Soil moisture modelling of a SMOS pixel: interest of using the PERSIANN database over the Valencia Anchor Station, *Hydrol. Earth Syst. Sci.*, 14, 1509–1525, doi:10.5194/hess-14-1509-2010, 2010.
- 5 Keyantash, J. and Dracup, A.: The quantification of drought: an evaluation of drought indices, *B. Am. Meteorol. Soc.*, 23, 1167–1180, 2002.
- Liang, X., Lettenmaier, D. P., Wood, E. F., and Burges, S. J.: A simple hydrologically based model of land-surface water and energy fluxes for general circulation models, *J. Geophys. Res.*, 99(D7), 14415–14428, 1994.
- 10 Liang, X., Wood, E. F., and Lettenmaier, D. P.: Surface soil moisture parameterization of the VIC-2L model: evaluation and modification, *Global Planet. Change*, 13, 195–206, 1996.
- Lievens, H., Verhoest, N. E. C., De Keyser, E., Verneeuwe, H., Matgen, P., Álvarez-Mozos, J., and De Baets, B.: Effective roughness modelling as a tool for soil moisture retrieval from C- and L-band SAR, *Hydrol. Earth Syst. Sci.*, 15, 151–162, doi:10.5194/hess-15-151-2011, 2011.
- 15 Loew, A. and Schlenz, F.: A dynamic approach for evaluating coarse scale satellite soil moisture products, *Hydrol. Earth Syst. Sci.*, 15, 75–90, doi:10.5194/hess-15-75-2011, 2011.
- Lobmeyr, M., Lohmann, D., and Ruhe, C.: An application of a large scale conceptual hydrological model over the Elbe region, *Hydrol. Earth Syst. Sci.*, 3, 363–374, doi:10.5194/hess-3-363-1999, 1999.
- 20 Ma, Z. G. and Fu, C. B.: Interannual characteristics of the surface hydrological variables over the arid and semi-arid areas of Northern China, *Global Planet. Change*, 37, 189–200, doi:10.1016/S0921-8181(02)00203-5, 2003.
- Ma, Z. G. and Ren, X. B.: Drying Trend over China from 1951 to 2006, *Adv. Clim. Change Res.*, 25 3(4), 195–201, 2007.
- McKee, T. B. N., Doesken, J., and Kleist, J.: The relationship of drought frequency and duration to time scales, Eight Conf. on Applied Climatology, Anaheim, CA, Am. Meteorol. Soc., 179–184, 1993.
- 30 Mo, K. C.: Model-based drought indices over the United States, *J. Hydrometeorol.*, 9, 1212–1230, 2008.
- Narasimhan, B. and Srinivasan, R.: Development and evaluation of soil moisture deficit index (SMDI) and evapotranspiration deficit index (ETDI) for agricultural drought monitoring, *Agr. Forest Meteorol.*, 133, 69–88, 2005.

Reconstructing and analyzing China's drought history (1951–2009)

Z. Y. Wu et al.

[Title Page](#)

[Abstract](#)

[Introduction](#)

[Conclusions](#)

[References](#)

[Tables](#)

[Figures](#)

◀

▶

[Back](#)

[Close](#)

[Full Screen / Esc](#)

[Printer-friendly Version](#)

[Interactive Discussion](#)



Nijssen, B., Schnur, R., and Lettenmaier, D. P.: Global retrospective estimation of soil moisture using the variable infiltration capacity land surface model, 1980–93, *J. Climate*, 14, 1790–1808, 2001.

Office of State Flood Control and Drought Relief Headquarters and Nanjing Institute of Hydrology and Water Resources, Ministry of Water Resources, China (Eds.): *China flood and drought disaster*, China WaterPower Press, Beijing, 569 pp., 1997.

Palmer, W. C.: Meteorological drought, *Weather Bureau, Research Paper No. 45*, US Dept. of Commerce, Washington, DC, 58 pp., 1965.

Palmer, W. C.: Keeping track of crop moisture conditions, nationwide: the new crop moisture index, *Weatherwise*, 21, 156–161, 1968.

Raziei, T., Bordi, I., and Pereira, L. S.: A precipitation-based regionalization for Western Iran and regional drought variability, *Hydrol. Earth Syst. Sci.*, 12, 1309–1321, doi:10.5194/hess-12-1309-2008, 2008.

Reynolds, C. A., Jackson, T. J., and Rawls, W. J.: Estimating soil water-holding capacities by linking the Food and Agriculture Organization soil map of the world with global pedon databases and continuous pedotransfer functions, *Water Resour. Res.*, 36, 3653–3662, 2000.

Richard, R. and Heim, J. R.: A review of twentieth century drought index used in the United States, *B. Am. Meteorol. Soc.*, 83, 1149–1165, 2002.

Sheffield, J., Goteti, G., Wen, F., and Wood, E. F.: A simulated soil moisture based drought analysis for the United States, *J. Geophys. Res.*, 109, D24108, doi:10.1029/2004JD005182, 2004.

Stephen, H., Ahmad, S., Piechota, T. C., and Tang, C.: Relating surface backscatter response from TRMM precipitation radar to soil moisture: results over a semi-arid region, *Hydrol. Earth Syst. Sci.*, 14, 193–204, doi:10.5194/hess-14-193-2010, 2010.

te Linde, A. H., Aerts, J. C. J. H., Hurkmans, R. T. W. L., and Eberle, M.: Comparing model performance of two rainfall-runoff models in the Rhine basin using different atmospheric forcing data sets, *Hydrol. Earth Syst. Sci.*, 12, 943–957, doi:10.5194/hess-12-943-2008, 2008.

Verseghy, D. L.: CLASS A Canadian land surface scheme for GCMS, I. Soil model, *Int. J. Climatol.*, 11, 111–133, 1991.

Verseghy, D. L., McFarlane, N. A., and Lazare, M.: CLASS A Canadian land surface scheme for GCMS, II. Vegetation model and coupled runs, *Int. J. Climatol.*, 13, 347–370, 1993.

Vicente-Serrano, S. M. and López-Moreno, J. I.: Hydrological response to different time scales

Reconstructing and analyzing China's drought history (1951–2009)

Z. Y. Wu et al.

- of climatological drought: an evaluation of the Standardized Precipitation Index in a mountainous Mediterranean basin, *Hydrol. Earth Syst. Sci.*, 9, 523–533, doi:10.5194/hess-9-523-2005, 2005.
- Wang, Z. W. and Zhai, P. M.: Climate change in drought over Northern China during 1950–2000, *Acta Geogr. Sin.*, supplement, 58, 61–68, 2003.
- Wen, K., Jin, G. S., and Li, D. J.: A mathematical model for catchment runoff calculation, *J. Hydraul. Eng.*, 13, 1–12, 1982.
- Wen, L., Wu, Z. Y., Lu, G. H., Lin, C. A., Zhang, J. Y., and Yang, Y.: Analysis and improvement of runoff generation in the land surface scheme CLASS and comparison with field measurements from China, *J. Hydrol.*, 345, 1–15, 2007.
- WMO: Drought and Agriculture, WMO Tech, Note 138, Geneva, Switzerland, 127 pp., 1975.
- Wu, Z. Y., Lu, G. H., Wen, L., Lin, C. A., Zhang, J. Y., and Yang, Y.: Thirty-five year (1971–2005) simulation of daily soil moisture using the variable infiltration capacity model over China, *Atmos. Ocean*, 45, 37–45, 2007.
- Zhai, J. Q., Su, B. D., and Krysanova, V.: Spatial variation and trends in PDSI and SPI indices and their relation to streamflow in 10 large regions of China, *J. Climate*, 23, 649–663, doi:10.1175/2009JCLI2968.1, 2010.
- Zhang, S. F., Su, Y. S., and Song, D. D.: China historical drought 1949–2000, Hohai University Press, Nanjing, 680 pp., 2008a.
- Zhang, W. Y.: On China drought disaster and mitigation measures, *disaster reduction in China*, 1, 47–49, 2003.
- Zhang, W. J., Zhou, T. J., and Yu, R. C.: Spatial distribution and temporal variation of soil moisture over China – Part I: Multi-data intercomparison, *Chinese J. Atmos. Sci.*, 32(3), 581–597, 2008b.
- Zhang, X. Y.: Analysis and assesment of soil moisture in China based on the situ observation data, Dissertation for the Master Degree, China University of Geosciences, Beijing, 77 pp., 2009.
- Zhao, R. J., Zhang, Y. L., Fang, L. R., Liu, X. R., and Zhang, Q. S.: The Xinanjiang model, in: *Hydrological Forecasting Proceedings Oxford Symposium*, IASH 129, 351–356, 1980.
- Zou, X. K., Zhai, P. M., and Zhang, Q.: Variations in droughts over China: 1951–2003, *Geophys. Res. Lett.*, 32, L04707, doi:10.1029/2004GL021853, 2005.
- Zuo, Z. Y. and Zhang, R. H.: Temporal and spatial variation of soil moisture in spring over Eastern China, *Sci. China Ser. D*, 11, 1428–1437, 2008.

[Title Page](#)

[Abstract](#)

[Introduction](#)

[Conclusions](#)

[References](#)

[Tables](#)

[Figures](#)

◀

▶

◀

▶

[Back](#)

[Close](#)

[Full Screen / Esc](#)

[Printer-friendly Version](#)

[Interactive Discussion](#)



Table 1. Soil moisture classifications based on the SMAPI (Soil Moisture Anomaly Percentage Index).

Category	SMAPI	Average Frequency
extreme drought	$\leq -50\%$	0.005
severe drought	-50% to -30%	0.020
moderate drought	-30% to -15%	0.100
mild drought	-15% to -5%	0.200
near normal	-5% to 5%	0.350
slightly wet	5% to 15%	0.200
moderately wet	15% to 30%	0.100
very wet	30% to 50%	0.020
extremely wet	$> 50\%$	0.005



Reconstructing and analyzing China's drought history (1951–2009)

Z. Y. Wu et al.

Table 2. The list of total regional drought events over China's nine drought study regions identified by the SMAPI-based procedure during the period 1951 to 2009, with the top three most severe drought events. The regional drought events sorted according to their severity. The beginning and ending dates (T_1/T_2) of a drought event are given, as well as the duration (D) and the drought areal extent (A).

Study regions	Total drought events	First ranking			Second ranking			Third ranking		
		T_1/T_2	D (d)	A (%)	T_1/T_2	D (d)	A (%)	T_1/T_2	D (d)	A (%)
Xinjiang	6	12 Sep 1956/23 Apr 1957	224	40.0	11 Oct 1997/24 Mar 1998	165	34.2	26 Oct 1955/2 Apr 1956	160	33.5
Tibet	25	22 Aug 1957/13 Oct 1960	1149	41.9	3 Jul 1994/30 Jun 1996	729	47.3	18 Jun 1952/3 Jul 1954	746	42.8
Northwest	26	27 May 1952/25 Jan 1954	609	51.0	22 Jun 2006/17 Jun 2007	361	46.7	10 Jul 2002/7 May 2003	302	48.7
Inner Mongolia	37	14 Jul 1999/10 Jun 2002	1063	61.0	29 Jun 2006/23 Jun 2008	726	64.1	1 Jul 2005/29 Jun 2006	364	74.2
Northeast	38	24 May 2000/19 Jun 2002	757	63.5	14 Aug 1977/19 Apr 1979	614	54.5	20 Jul 1967/28 Sep 1968	437	64.0
North	53	27 Aug 1998/22 Oct 2000	788	75.1	29 Jul 1991/3 May 1994	1010	59.8	7 Jul 1980/21 Jun 1982	715	72.8
East	46	16 Jun 1978/6 May 1979	325	68.9	15 Jul 1966/5 Mar 1967	234	65.2	22 Jul 1992/14 Jan 1993	177	67.2
Southwest	41	15 Jun 2006/1 Feb 2007	232	53.6	30 Jul 2003/7 Apr 2004	253	45.3	10 Jan 1963/22 Aug 1963	225	48.3
South	53	20 Sep 1954/31 May 1955	254	80.7	21 Sep 2003/22 Jul 2004	306	70.2	9 Dec 1962/24 Jul 1963	228	73.2

- [Title Page](#)
- [Abstract](#) [Introduction](#)
- [Conclusions](#) [References](#)
- [Tables](#) [Figures](#)
- [◀](#) [▶](#)
- [◀](#) [▶](#)
- [Back](#) [Close](#)
- [Full Screen / Esc](#)
- [Printer-friendly Version](#)
- [Interactive Discussion](#)



**Reconstructing and
analyzing China's
drought history
(1951–2009)**

Z. Y. Wu et al.

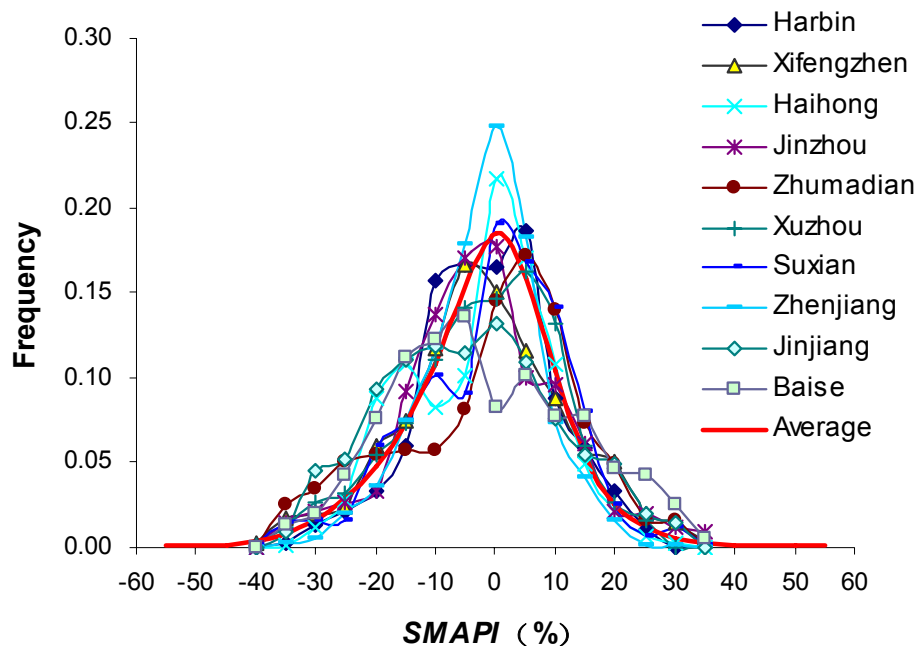


Fig. 1. The frequency distributions of SMAPI (Soil Moisture Anomaly Percentage Index; see text for discussion) for 10 Chinese experimental sites together with their average.

- [Title Page](#)
- [Abstract](#) [Introduction](#)
- [Conclusions](#) [References](#)
- [Tables](#) [Figures](#)
- [◀](#) [▶](#)
- [◀](#) [▶](#)
- [Back](#) [Close](#)
- [Full Screen / Esc](#)
- [Printer-friendly Version](#)
- [Interactive Discussion](#)

Reconstructing and analyzing China's drought history (1951–2009)

Z. Y. Wu et al.

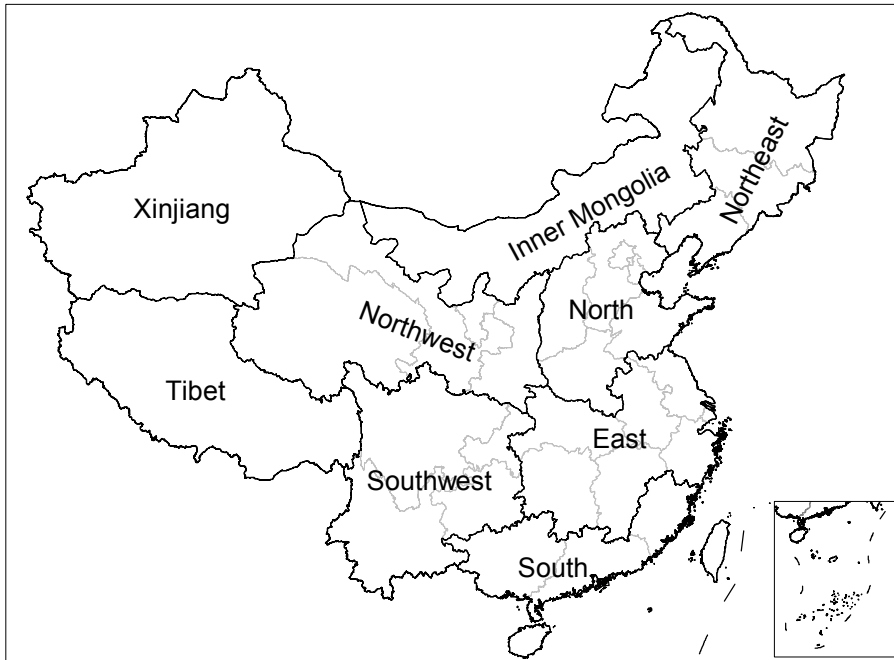


Fig. 2. The geographical distribution of China's nine drought study regions and provinces. The black solid lines delineate the drought study regions, while the gray lines are the boundary of provinces.

Discussion Paper | Discussion Paper

Discussion Paper | Discussion Paper

Discussion Paper | Discussion Paper

[Title Page](#)

[Abstract](#)

[Introduction](#)

[Conclusions](#)

[References](#)

[Tables](#)

[Figures](#)



[Back](#)

[Close](#)

[Full Screen / Esc](#)

[Printer-friendly Version](#)

[Interactive Discussion](#)

Reconstructing and analyzing China's drought history (1951–2009)

Z. Y. Wu et al.

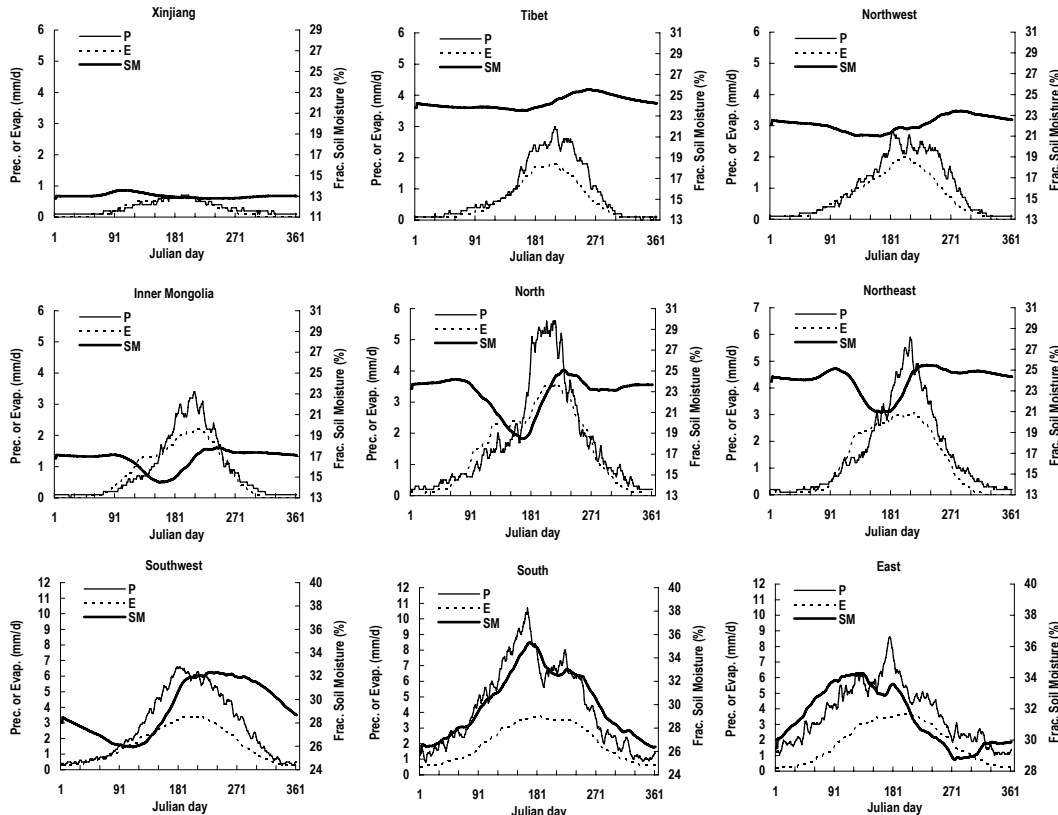


Fig. 3. The annual cycle of VIC soil moisture (SM: thick solid line) for the period 1951–2009 over China's nine drought study regions, as well as the observed precipitation (P: thin solid line) and the simulated evapotranspiration (E: dashed line).

Title Page

Abstract

Introduction

Conclusions

References

Tables

Figures



Full Screen / Esc

Printer-friendly Version

Interactive Discussion

**Reconstructing and
analyzing China's
drought history
(1951–2009)**

Z. Y. Wu et al.

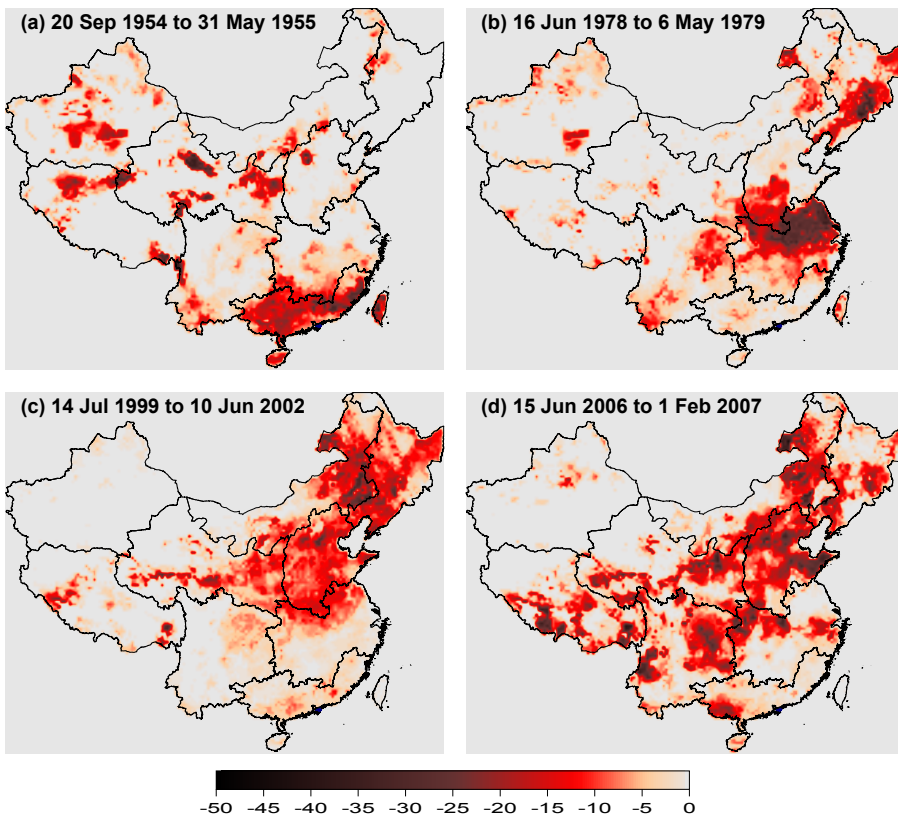


Fig. 4. Four reconstructed most severe drought events together with other drought-affected areas for the same events during the period 1951–2009.

[Title Page](#)[Abstract](#)[Introduction](#)[Conclusions](#)[References](#)[Tables](#)[Figures](#)[◀](#)[▶](#)[◀](#)[▶](#)[Back](#)[Close](#)[Full Screen / Esc](#)[Printer-friendly Version](#)[Interactive Discussion](#)

Reconstructing and analyzing China's drought history (1951–2009)

Z. Y. Wu et al.

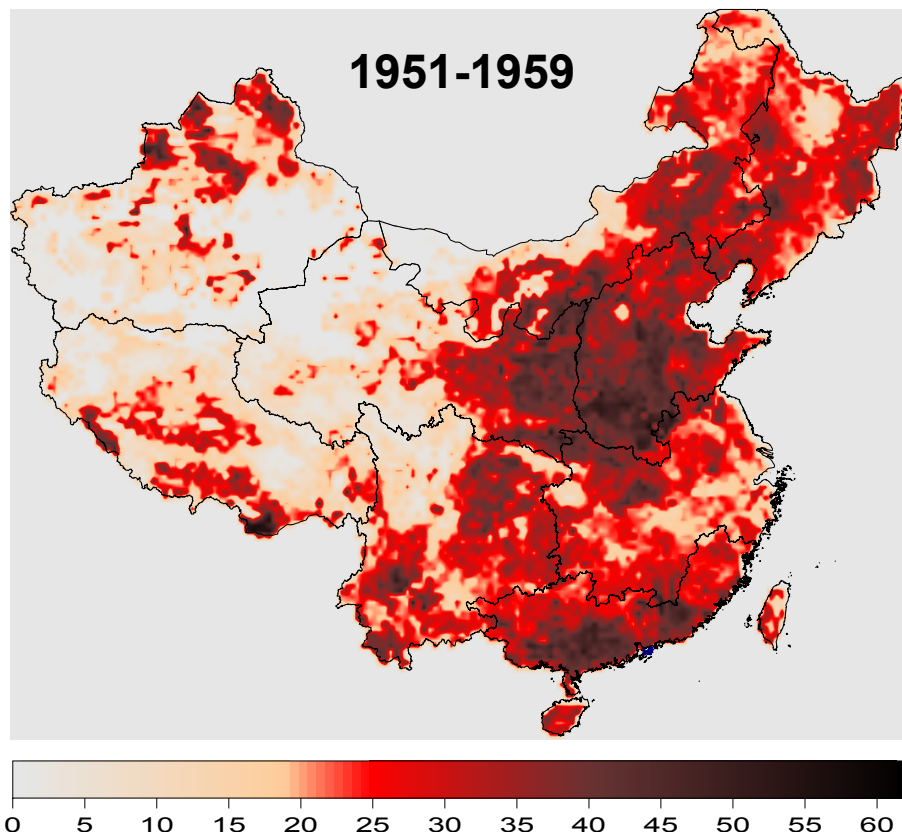


Fig. 5. The geographic distribution of drought occurrence times over China for the period 1951–2009.

**Reconstructing and
analyzing China's
drought history
(1951–2009)**

Z. Y. Wu et al.

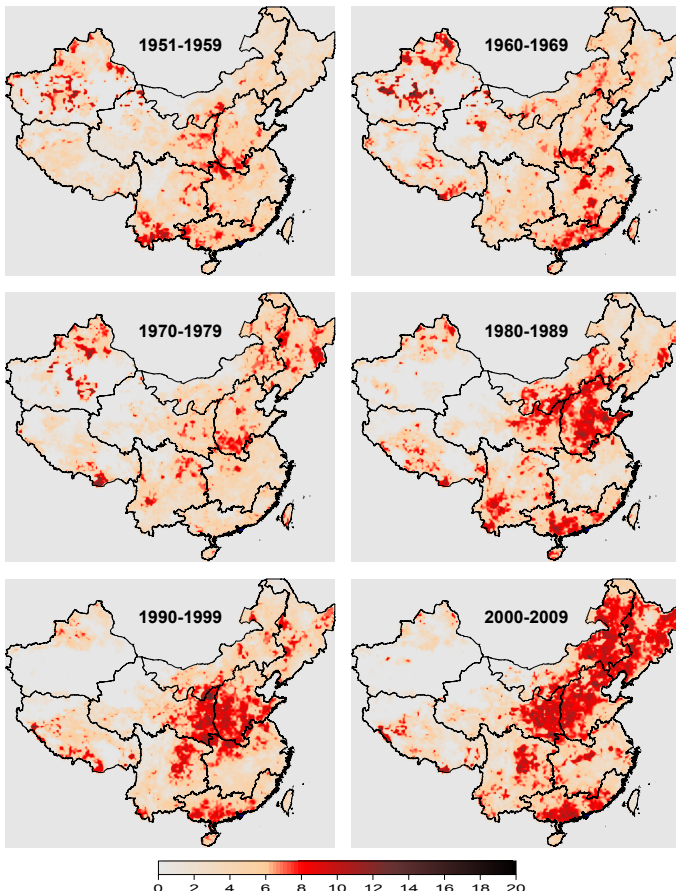


Fig. 6. The geographic distributions of drought occurrence times over China for the six decadal periods, 1951–1959, 1960–1969, 1970–1979, 1980–1989, 1990–1999 and 2000–2009.

[Title Page](#)[Abstract](#)[Introduction](#)[Conclusions](#)[References](#)[Tables](#)[Figures](#)[Back](#)[Close](#)[Full Screen / Esc](#)[Printer-friendly Version](#)[Interactive Discussion](#)

Reconstructing and analyzing China's drought history (1951–2009)

Z. Y. Wu et al.

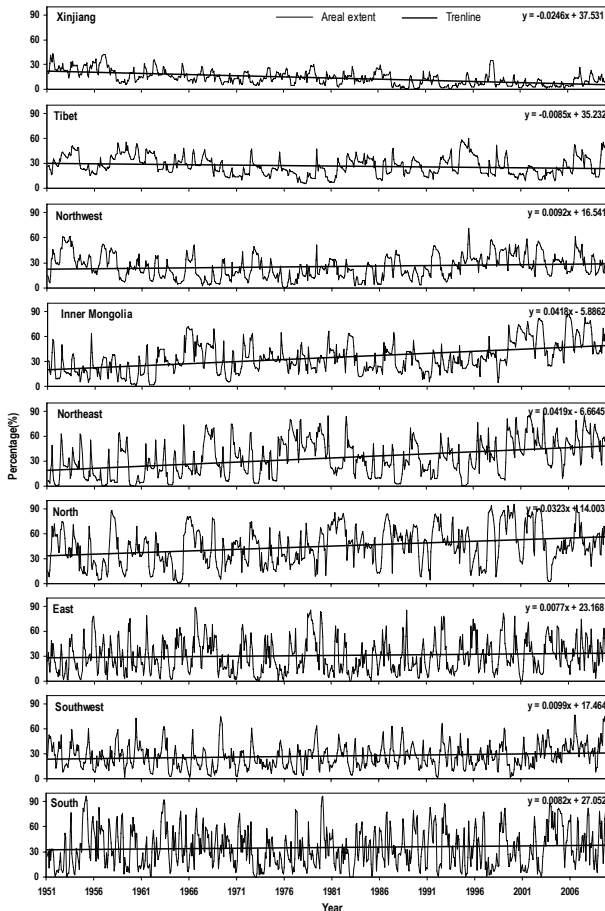


Fig. 7. Time series of the monthly areal extent of drought for 1951–2009. The areal extent is calculated as the month mean percentage area of the division for which the daily grid's SMAP (%) is less than -5% . The subplots correspond to China's nine drought study regions.

[Title Page](#)

[Abstract](#)

[Introduction](#)

[Conclusions](#)

[References](#)

[Tables](#)

[Figures](#)

◀

▶

◀

▶

[Back](#)

[Close](#)

[Full Screen / Esc](#)

[Printer-friendly Version](#)

[Interactive Discussion](#)

Reconstructing and analyzing China's drought history (1951–2009)

Z. Y. Wu et al.

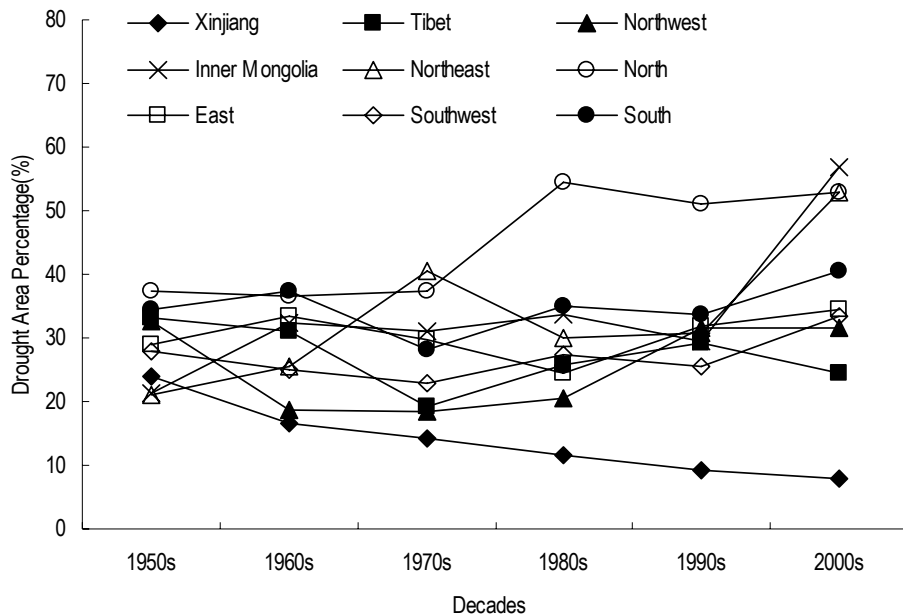


Fig. 8. Decadal average of drought area percentages on the nine drought study regions. The six decades are 1950s (1951–1959), 1960s (1960–1969), 1970s (1970–1979), 1980s (1980–1989), 1990s (1990–1999) and 2000s (2000–2009).

- [Title Page](#)
- [Abstract](#) [Introduction](#)
- [Conclusions](#) [References](#)
- [Tables](#) [Figures](#)
- [◀](#) [▶](#)
- [◀](#) [▶](#)
- [Back](#) [Close](#)
- [Full Screen / Esc](#)

[Printer-friendly Version](#)

[Interactive Discussion](#)